Supplemental Figures

Does $\delta^{18}O$ of O_2 record meridional shifts in tropical rainfall?

Alan M. Seltzer,[1] Christo Buizert[2], Daniel Baggenstos[3], Edward J. Brook[2], Jinho Ahn[4], Ji-Woong Yang[4], Jeffrey P. Severinghaus[1]

[1]Scripps Institution of Oceanography, University of California-San Diego, La Jolla, CA, 92037, USA
[2]College of Earth, Ocean and Atmospheric Sciences, Oregon State University, Corvallis, OR, 97331, USA
[3]Climate and Environmental Physics, University of Bern, Bern, 3012, Switzerland
[4]School of Earth and Environmental Sciences, Seoul National University, Seoul, 08826, South Korea

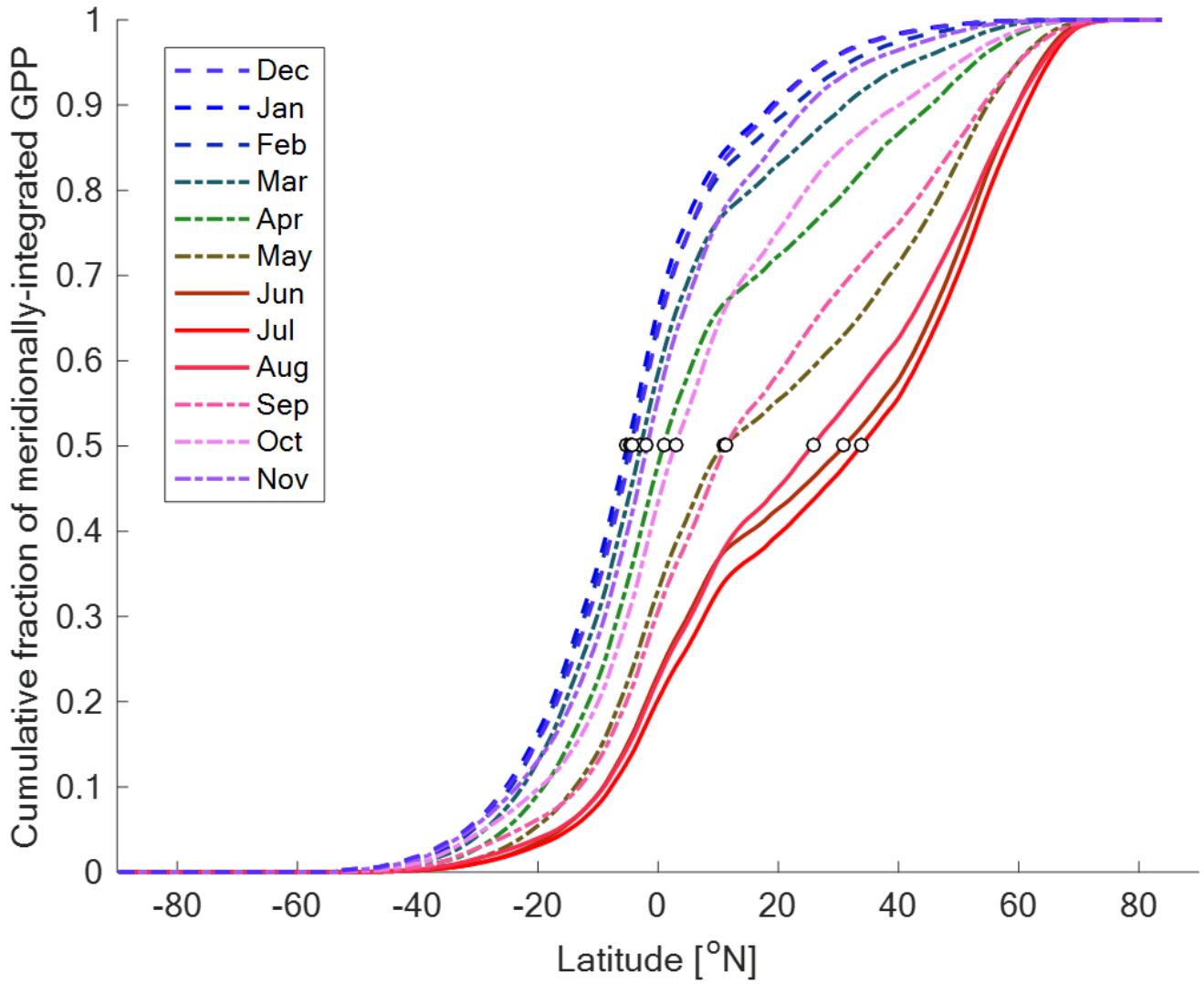

Figure S1: Cumulative, meridionally integrated fraction of global monthly GPP versus latitude, used to determine centroid latitude of terrestrial oxygenesis (TOE).

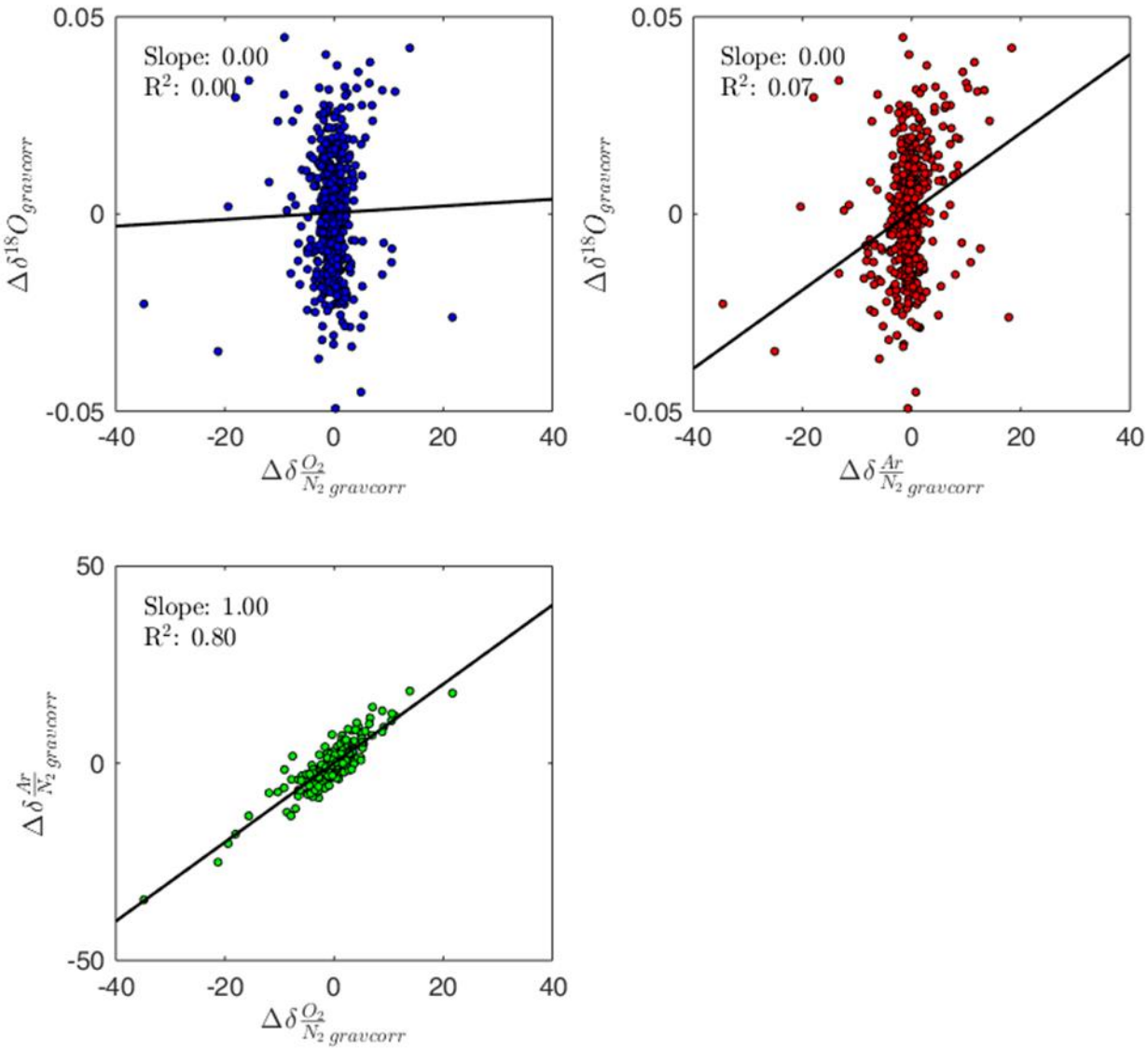

Figure S2: WAIS Divide replicate pair differences (Δδ) in gravitationally corrected $\delta^{18}O$, $\delta O_2/N_2$, and $\delta Ar/N_2$.

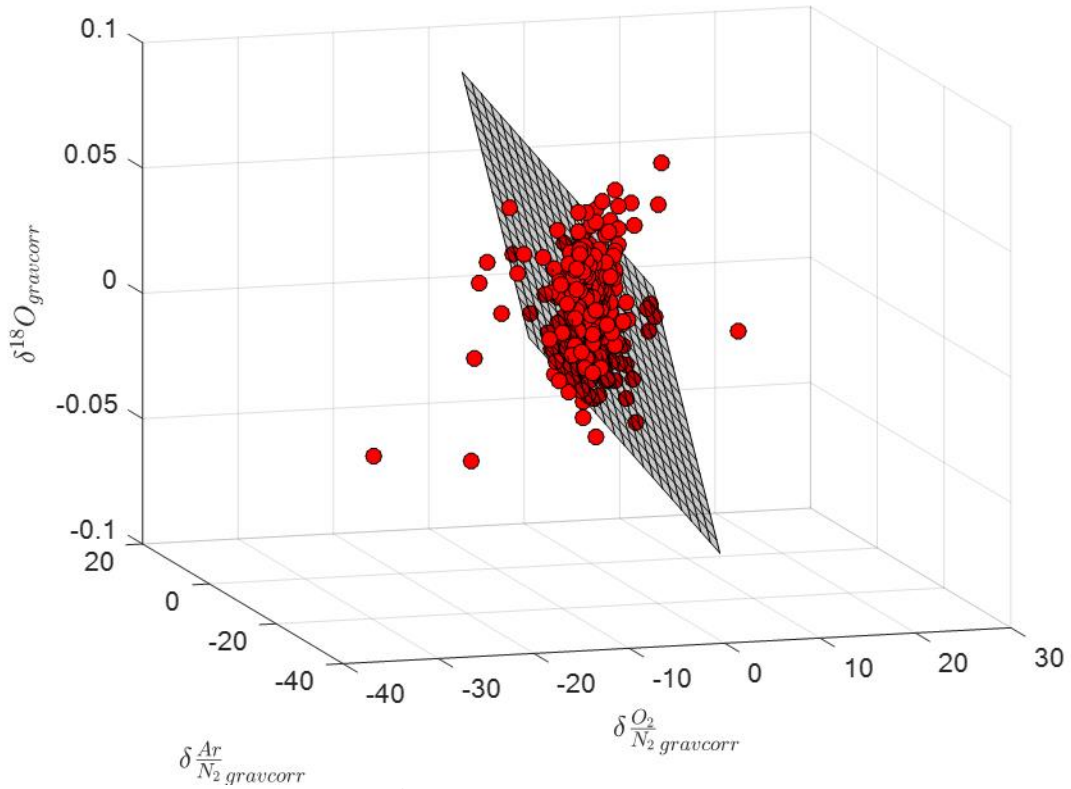

Figure S3: Plane of best fit (R^2=0.31) for WAIS Divide replicate pair differences (Δδ) of gravitationally corrected $\delta^{18}O$, $\delta O_2/N_2$, and $\delta Ar/N_2$.

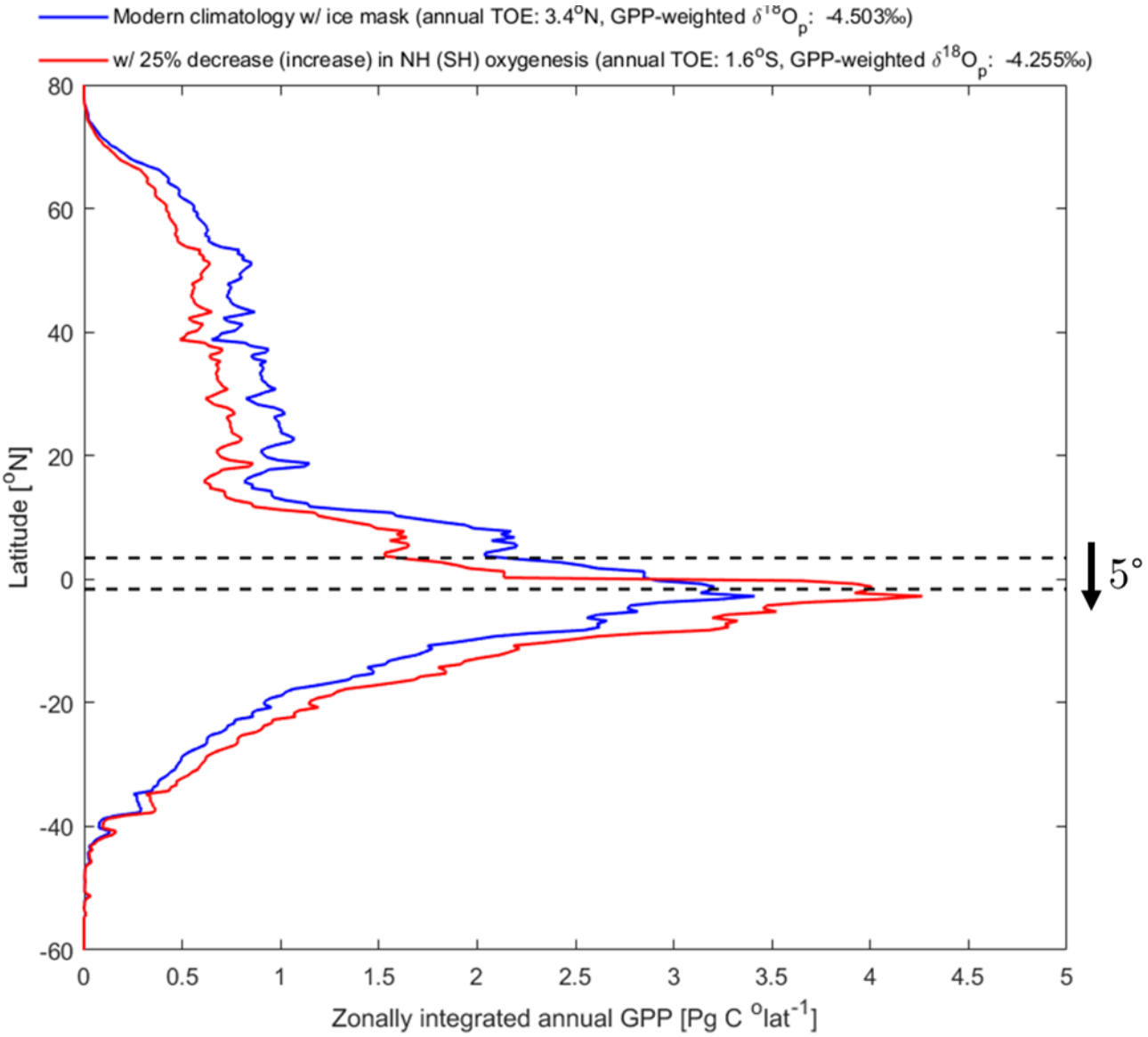

Figure S4: Results of TOE-$\delta^{18}O_{precip}$ experiment to roughly estimate the scale of a $\Delta\varepsilon_{LAND}$ change for southward shift of oxygen production during Heinrich stadial. To loosely simulate background glacial conditions, a 26-ka ice mask (Argus et al., 2014) was overlain on the modern distributions of GPP and $\delta^{18}O_{precip}$ (i.e. GPP was zeroed out over glaciated regions). The blue curve shows the meridional distribution of GPP for this background glacial climatology. The red curve shows the results of reducing and increasing GPP uniformly by 25% over the Northern and Southern Hemispheres, respectively. The resulting 5° southward shift of the TOE is accompanied by a ~0.25‰ increase in GPP-weighted mean annual $\delta^{18}O_{precip}$.

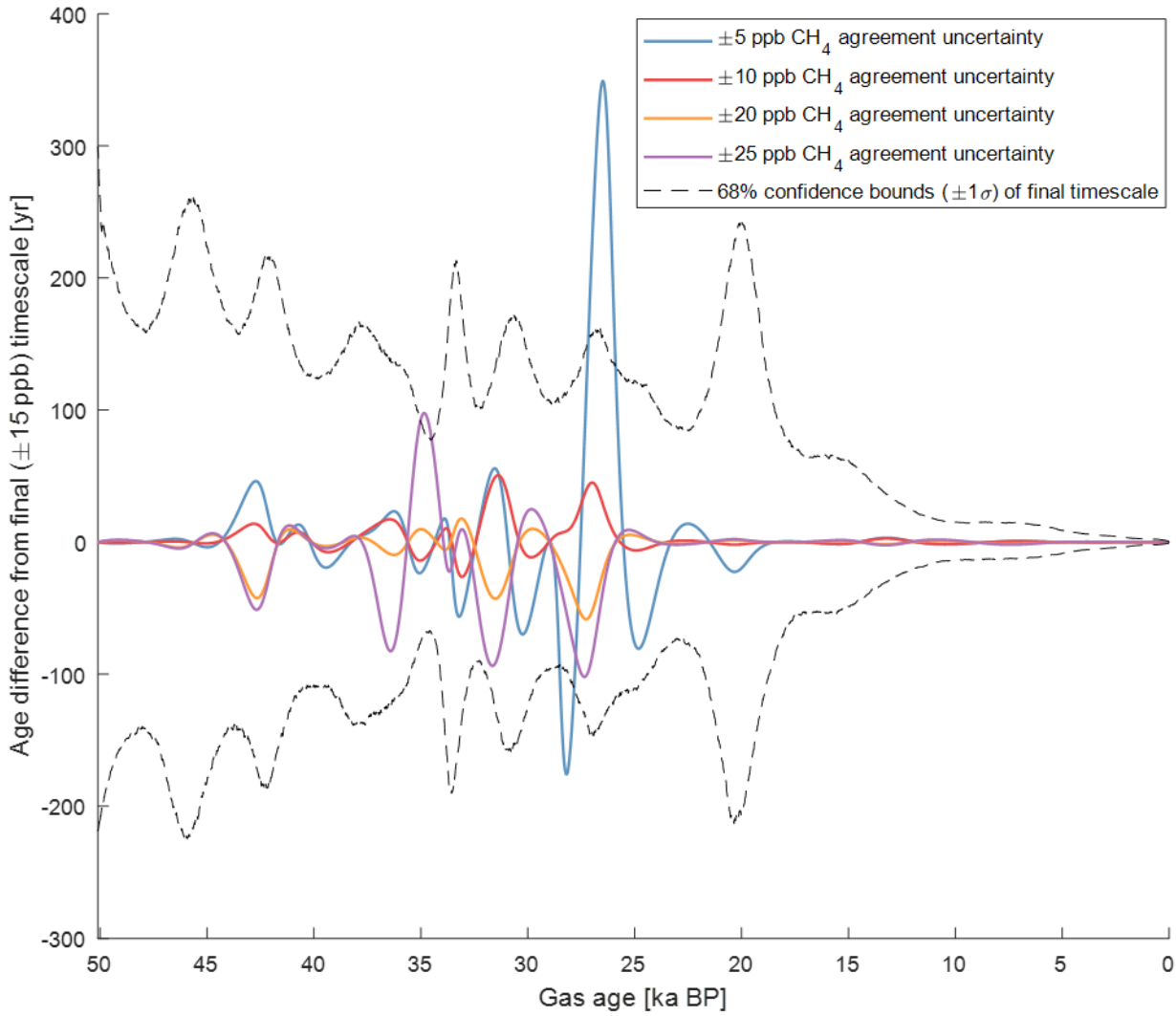

Figure S5: Results of CH_4 matching-window sensitivity test described in Appendix B, showing the deviation of each alternate timescale from the final timescale used in this study (i.e. Figure 2). The final timescale assumes a value matching range of ±15 ppb for CH_4 tie points. Each of these alternate timescales was estimated with CH_4 matching ranges varying from ±5-25 ppb. Alternate timescales with CH_4 ranges between ±10-20 ppb (red and orange curves) agree with the final (±15 ppb) timescale within ±1σ at all times (maximum absolute deviation ~58 years).

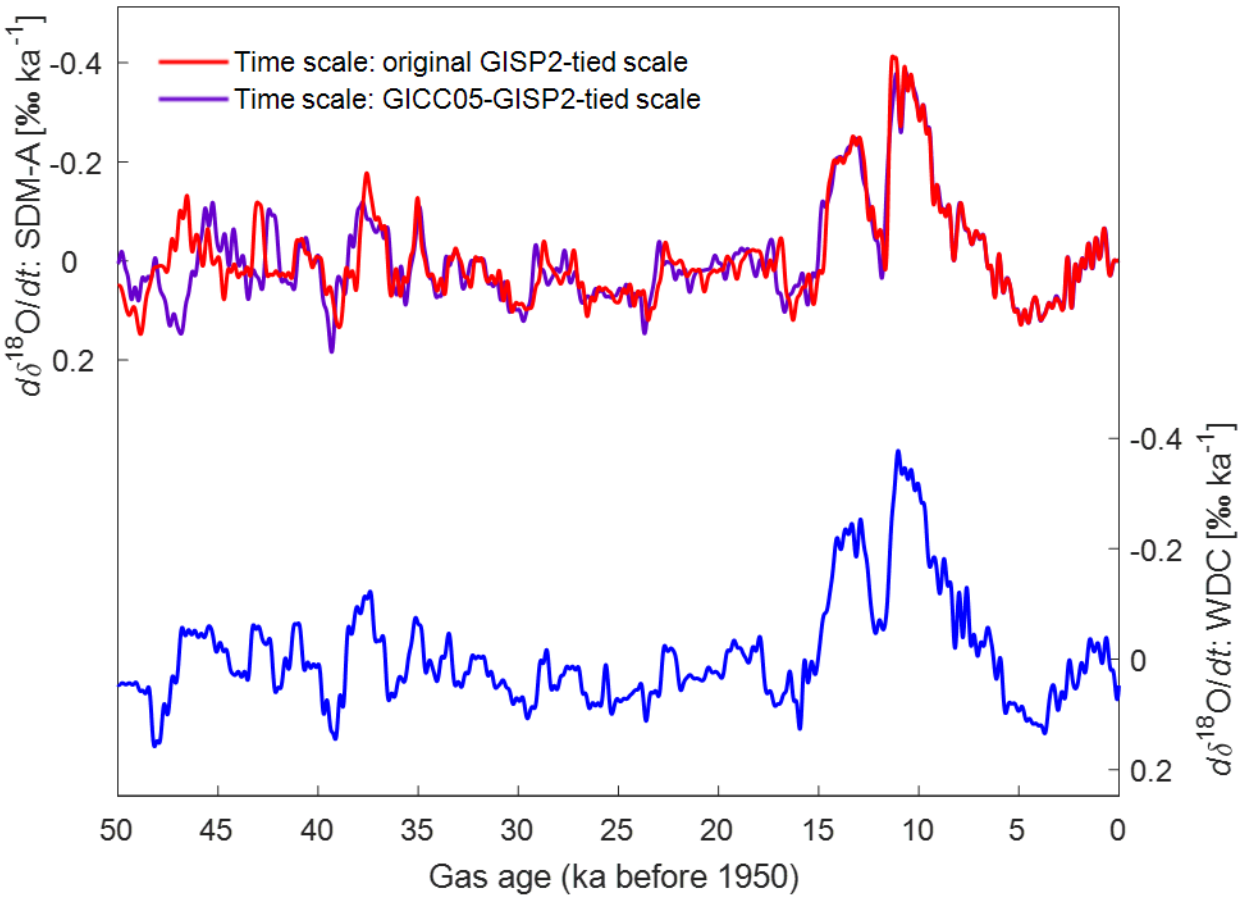

Figure S6: SD $d\delta^{18}O_{atm}/dt$ on the original *Brook et al.* (2005) timescale (red) and the alternate GISP2-tied GICC05 timescale (purple) and WD $d\delta^{18}O_{atm}/dt$ on the WD2014 timescale.

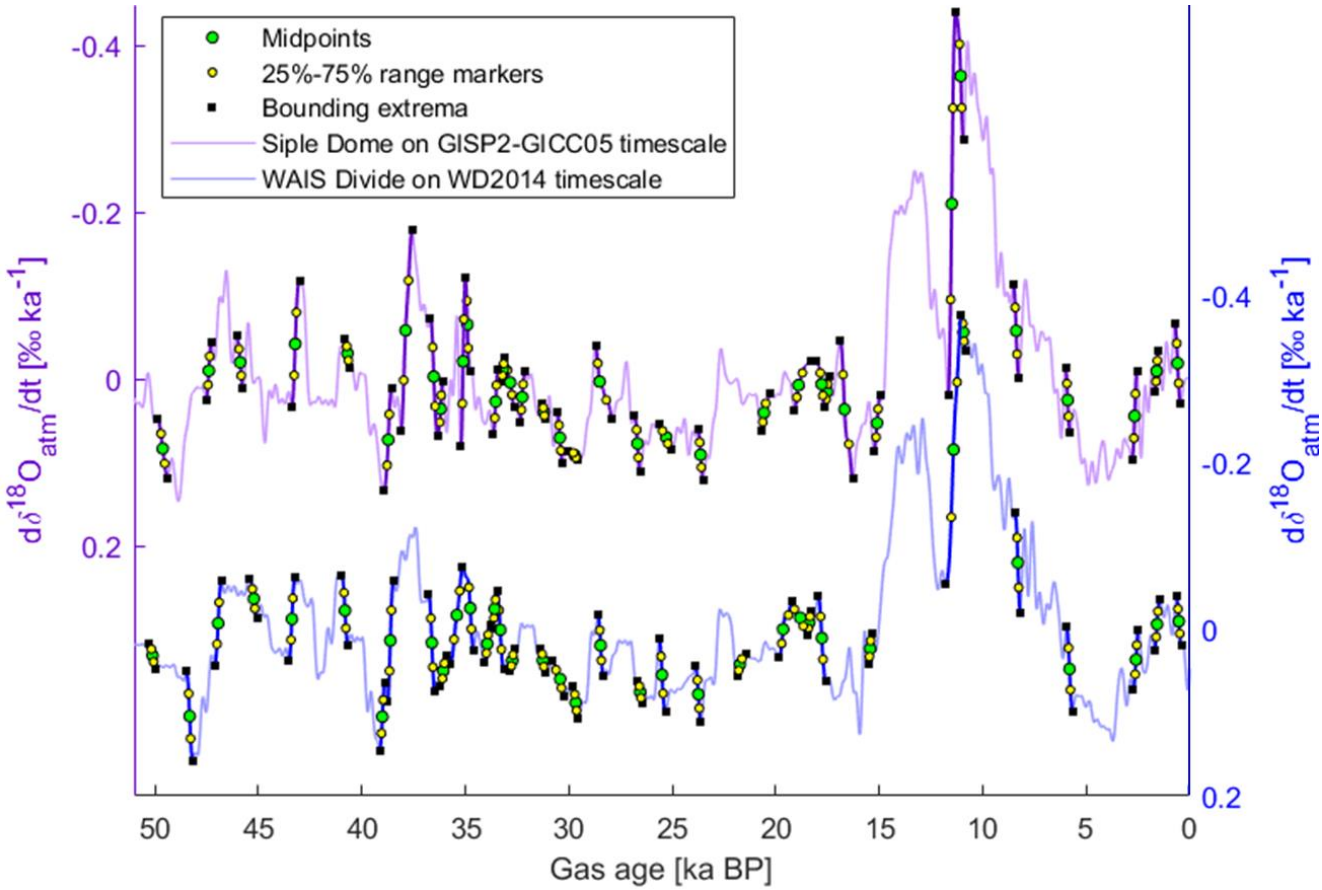

Figure S7: Overview of tie point selection process from $d\delta^{18}O_{atm}/dt$ records at WD (blue) and SD (red, on alternate GISP2-tied gas timescale). Green circles (N=36) indicate midpoints of abrupt $d\delta^{18}O_{atm}/dt$ transitions recorded in both records. Smaller yellow markers indicate 25% and 75% values between local extrema (black dots) bounding each abrupt transition. ±1σ tie point uncertainty was taken from the range of 25-75% markers.

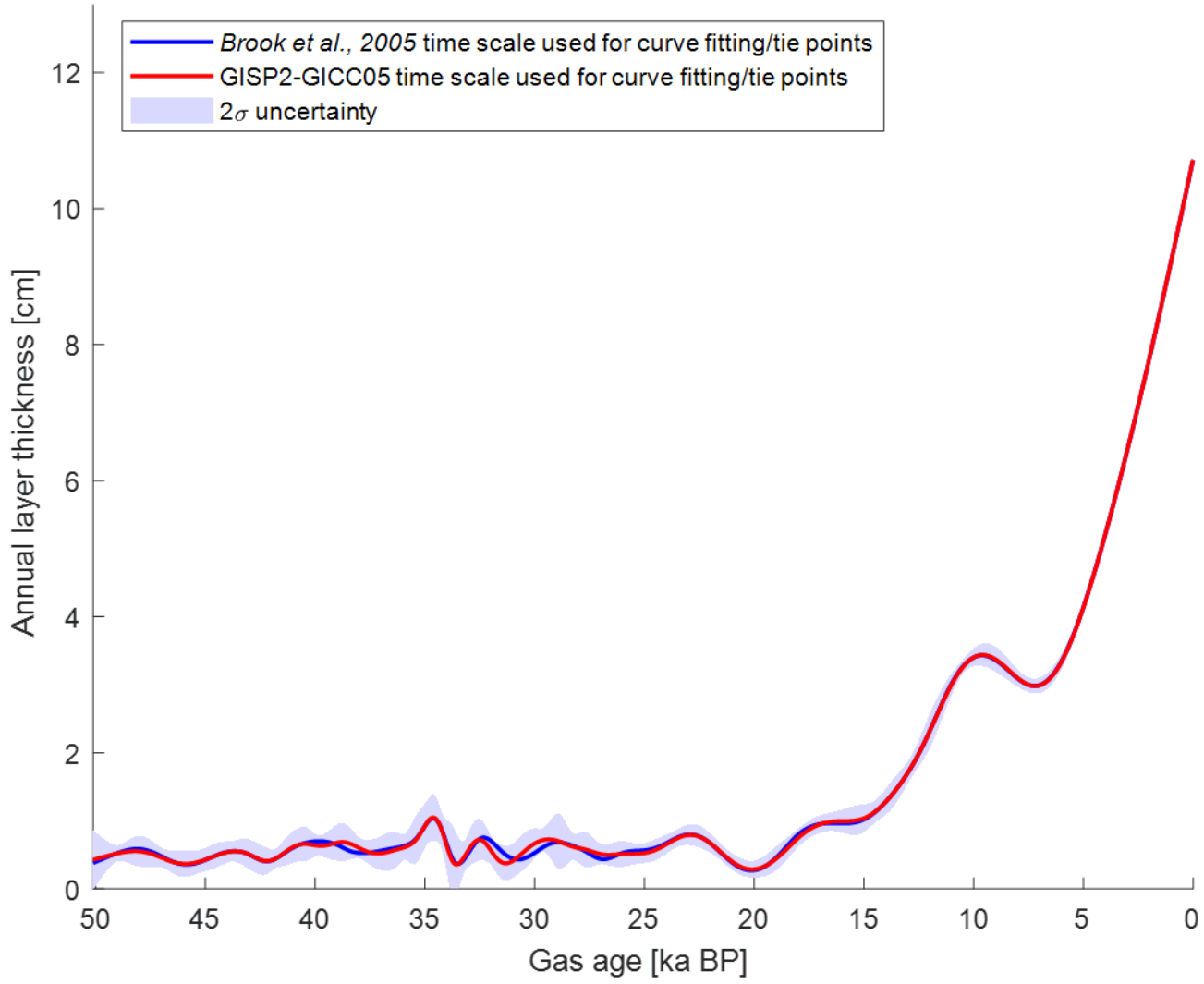

Figure S8: Annual layer thickness profiles estimated by ALT method using tie points derived from original *Brook et al.* (2005) SD timescale (blue line and shaded 2σ uncertainty) and alternate GICC05-based SD timescale (red line).